Apollonius unilateral transducer constant power gain circles on 3D Smith charts

A.A. Muller, E. Sanabria-Codesal, A. Moldoveanu, V. Asavei, P. Soto, V.E. Boria and S. Lucyszyn

Unilateral transducer constant power gain circles play an essential role in the design of radio-frequency amplifiers and active modulators, as they help to determine optimal impedance matching conditions to meet gain and stability specifications. It is shown that these gain circles are a subfamily of Apollonius circles. For better visualisation, unilateral transducer constant gain power circles have been plotted for the first time on the three-dimensional (3D) Smith chart. To this end, a natural relationship from an inversive geometry was required, in order to relate the gain circles with cutting planes for the 3D Smith chart.

Introduction: In the design of radio-frequency (RF) amplifiers and active modulators (e.g. frequency multipliers, mixers and small-shift frequency translators), the unilateral transducer constant power gain circles represent the loci of source and load impedances on a conventional two-dimensional (2D) Smith chart [1]. Constant input and output impedance mismatch circles have also been recently introduced [2]; these are slightly different to gain circles, but share the same geometrical properties. Displaying power levels, or observing the Smith chart coverage [3] for a specific power level, leads to poor visualisation when using 2D plots; gain and mismatch circles always converge to point circles (i.e. circles of zero radius) on the 2D Smith chart [1, 2].

Ellipses, hyperbolas and Apollonius circles are a set of points defined by two other points. On an ellipse, the sum of the distances to these two points is constant, whereas on a hyperbola, the difference is constant. In the case of Apollonius circles, the ratio of the distances to these two points is constant [4], as seen in Fig. 1.

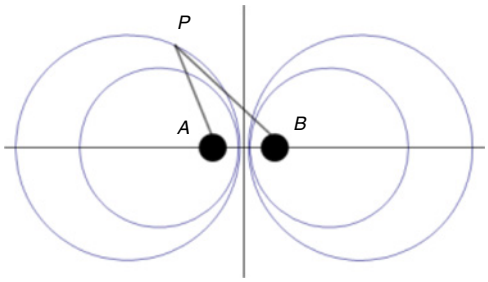

Fig. 1 *Circles of Apollonius, with respect to points A and B: PA/PB ratio is constant for any point P on circle (two reciprocal pairs of Apollonius circles are plotted)*

A and *B* are considered point circles, corresponding to a ratio of zero and infinity, respectively [4]

The concept of an Apollonius gasket for a microwave antenna design was recently introduced [5]. In this Letter, we focus on the unilateral transducer constant power gain circle equations [1] and prove that they are a subfamily of Apollonius circles. As a result, the convergence of these gain circles to specific points on the Smith chart plane is not a matter of chance and, thus, it will be shown that the source and load impedances also share other geometrical properties.

Finally, the 3D Smith chart concept (based on the Riemann sphere) and associated Java tools, recently introduced by Muller *et al.* [6, 7], are extended to plot gain circles using the unit sphere.

Gain circles on 2D Smith chart: The unilateral transducer power gain for a 2-port network G_{TU} is given by the following textbook equations [1]:

$$G_{TU} = G_S \cdot G_O \cdot G_L;\ \ G(\text{dB}) = 10\log_{10}(G) \tag{1}$$

where the respective intrinsic power gain factors associated with the source input stage, forward transmissions of the transducer and load output stage are

$$G_S = \frac{1-|\Gamma_s|^2}{|1-S_{11}\cdot\Gamma_s|^2};\ \ G_O = |S_{21}|^2;\ \ G_L = \frac{1-|\Gamma_L|^2}{|1-S_{22}\cdot\Gamma_L|^2} \tag{2}$$

At the input stage, Γ_s is the voltage-wave reflection coefficient of the source impedance, whereas S_{11} represents the input voltage-wave reflection coefficient of the 2-port network. Moreover, S_{21} is the forward voltage-wave transmission coefficient of the 2-port network, whereas its reverse voltage-wave transmission coefficient S_{12} is assumed to be zero. Finally, at the output stage, Γ_L is the voltage-wave reflection coefficient of the load impedance, whereas S_{22} represents the output voltage-wave reflection coefficient of the 2-port network. It should be noted that with purely passive stages/transducer the associated power gain factor $0 \le G \le 1$ and $-\infty \le G(\text{dB}) \le 0$, whereas active circuits [8, 9] can extend this range beyond the unity to $0 \le G \le \infty$ and $-\infty \le G(\text{dB}) \le +\infty$.

For convenience, only the gain circles associated with the input stage will be considered further, as the same approach applies to the output stage. Plotting G_S gives the gain circles in the complex Γ_S-plane, contribution to the unilateral transducer power gain. As an example, consider a commercially available transistor (BFP 405 from Infineon Technologies AG), having measured values of magnitude and phase for S_{11} of 0.707 and $-67°$, respectively, at 1900 MHz [1]. Fig. 2 shows the resulting family of source gain circles.

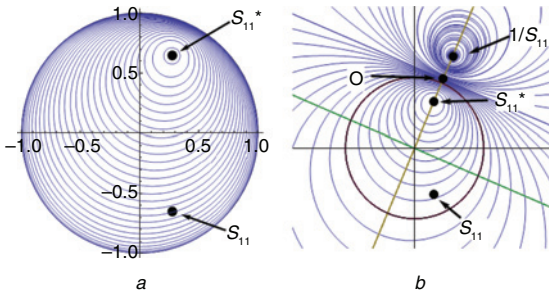

Fig. 2 *Unilateral transducer constant power gain circles using (2), ($G_O = G_L = 1$ for illustration purposes) for $S_{11} = (0.707,\ -67°)$ with $G_S \ge 0$ or $G_s(\text{dB}) \ge -\infty$ (Fig. 2a) and complete family $-\infty \le G_S \le +\infty$ (including fictitious case $G_S \le 0$) (Fig. 2b)*

Gain circles associated with positive values for source input power gain factor G_S are contained in the conventional 2D Smith chart, as seen in Fig. 2*a*. Note that, according to (2), the gain circle associated with $G_S = 0$ (i.e. $G_S(\text{dB}) = -\infty$) coincides with the Smith chart contour $|\Gamma_S| = 1$. Moreover, positive G_S gain circles converge to the point circle positioned at S_{11}^* (i.e. the complex conjugate of S_{11}) in the complex Γ_S-plane, which provides the maximum source input power gain factor [1]. However, after also plotting the negative G_S gain circles, it is observed that there is convergence to the accumulation point $1/S_{11}$, corresponding to $G_s = -\infty$ (see Fig. 2*b*).

The equations for any point P in the Γ_S-plane moving along the Apollonius circles related to $A = S_{11}^*$ and $B = 1/S_{11}$ are given from Fig. 1 by Brannan *et al.* [4]

$$PA = m \times PB \tag{3}$$

with $m > 0$ or equivalently (considering the point $P = \Gamma_S$)

$$|\Gamma_s - S_{11}^*|^2 = m^2|\Gamma_s - 1/S_{11}|^2 \tag{4}$$

which corresponds to the equation of a circle of radius R and centre C

$$R = \frac{m}{|m^2-1|}|S_{11}^* - 1/S_{11}|;\quad C = \frac{m^2/S_{11} - S_{11}^*}{m^2-1} \tag{5}$$

The Apollonius circles derived here are now compared with the unilateral transducer constant power gain circles, whose radius and centre are [1]

$$R = \frac{\sqrt{1+(|S_{11}|^2-1)G_s}}{|1+|S_{11}|^2 G_s|};\quad C = \frac{G_s S_{11}^*}{1+G_s|S_{11}|^2} \tag{6}$$

Equating the expressions in (5) and (6) for the circle centres, the distance ratio m can be expressed in terms of G_S as

$$m = |S_{11}|\sqrt{1+G_s(|S_{11}|^2-1)} \tag{7}$$

It is important to note that (7) unifies the family of centre locations with

the same radii and, thus, the families represented by (5) and (6) will coincide. In our particular case, points A and B are given by (0.27625, 0.65080) and (0.55263, 1.30199), respectively; point O is therefore (0.41446, 0.97639), which is placed in the infinite line obtained when the denominator of R in (5) or (6) vanishes (i.e. where $m = 1$). This gives the solution $G_s = -2$ for the infinite line. The gain circles range from $G_S = 0$ to $G_S = 1/(1 - |S_{11}|^2) = 1.9994$ (i.e. between $-\infty$ and +3 dB). Considering (7), this means that m varies between $|S_{11}|$ and 0 and, thus, for any possible source impedance at point P, one can choose $A = S_{11}^*$, $B = 1/S_{11}$ and after varying m between 0 and $|S_{11}|$ using (3) the entire family of unilateral (source) power gain circles can be obtained.

Gain circles on 3D Smith chart: To exploit the recently proposed 3D Smith chart tool, a new representation for the power levels is given that overcomes the drawbacks associated with 2D visualisations [1, 3, 10].

Starting with the example given in the preceding Section, if one wishes to express the unilateral transducer power gain associated with each gain circle defined by (2), the 0 dB unilateral transducer power gain will be found when the gain circle passes through the centre of the 2D Smith chart (north pole – on the 3D Smith chart), whereas in our example a +3 dB unilateral transducer power gain will be found for a gain circle having a centre point at S_{11}^*. This can be seen in Fig. 3, whereas Fig. 4 shows the entire range of gain circles.

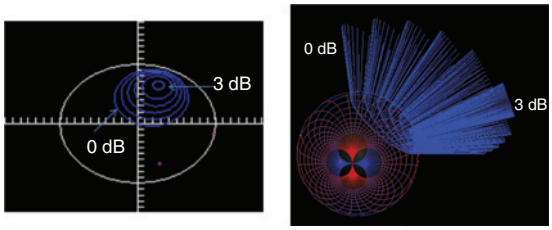

Fig. 3 *Unilateral transducer constant power gain circles using (2) (with $G_O = G_L = 1$ for illustration purposes) for $S_{11} = (0.707, -67°)$, $0 \le G_S$ (dB) $\le +3$ (i.e. only part of family)*

a 2D
b 3D

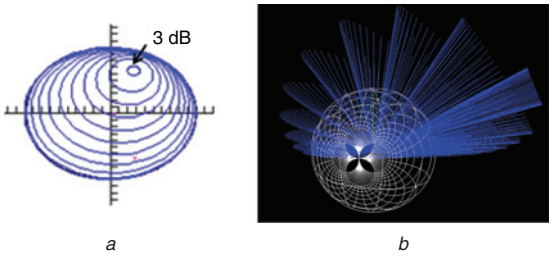

Fig. 4 *Expanded view of Fig. 3 for $S_{11} = (0.707, -67°)$, $(-\infty \le G_S$(dB) $\le +3)$*

a 2D
b 3D

Mathematical observation: Since the gain circles are a subfamily of the Apollonius circles, it can be proven that while plotting these on the 3D Smith chart their cutting planes will always meet on the infinite line for each value of S_{11} and, thus, on the axes of symmetry for the Apollonius circles. This can be seen in Fig. 5.

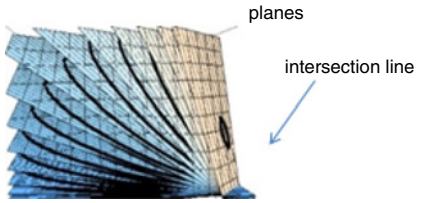

Fig. 5 *Symmetry axes of Apollonius circles when seen on 3D Smith chart, showing gain circles' meeting line*

Each gain circle corresponds to a cutting plane defined by (8), with a and b being the real and imaginary parts of S_{11}, respectively

$$2(ax + by)G_s + (2 + (|S_{11}|^2 - 1)G_s)z = (1 + |S_{11}|^2)G_s \quad (8)$$

Conclusion: It has been shown that unilateral transducer constant power gain circles (for the source input in our example) are a subfamily of the Apollonius circles, with respect to S_{11}^* and $1/S_{11}$. These gain circles have been plotted on the 3D Smith chart for the first time, as a newly proposed visualisation tool, overcoming traditional limits associated with contour plots on the traditional 2D Smith chart. It is interesting to note that unilateral transducer constant power gain circles are not the only Apollonius circles found in the RF theory. Indeed, the concept described here can also be applied for the design of antennas [10] and provide mismatch and noise figure circles, among others.

Acknowledgments: This work has been partly funded by the FP7 PCIG11-2012-322162 Marie Curie CIG, POSDRU/159/1.5/S/134398 and by DGCYT grant MTM2012-33073.

25 July 2014
doi: 10.1049/el.2014.2695
One or more of the Figures in this Letter are available in colour online.

A.A. Muller, P. Soto and V.E. Boria (*Microwave Applications Group, iTEAM, Universidad Politehnica de Valencia, Valencia, Spain*)

E-mail: andrei.stefan1@gmail.com

E. Sanabria-Codesal (*Departamento de Matemática Aplicada, Universitat Politècnica de València, Valencia, Spain*)

A. Moldoveanu and V. Asavei (*Faculty of Automatic Control and Computers, University Politehnica Bucuresti, Bucharest, Romania*)

S. Lucyszyn (*Department of Electrical and Electronic Engineering, Imperial College London, Exhibition Road, London, SW7 2AZ, United Kingdom*)

References

1 Gilmore, R., and Besser, L.: 'Practical RF circuit design for modern wireless systems – active circuits and systems' (Artech House, 2003), Vol. 2
2 Ciccognani, W., Longhi, P.E., Colangeli, S., and Limiti, E.: 'Constant mismatch circles and application to low-noise microwave amplifier design', *IEEE Trans. Microw. Theory Tech.*, 2013, **61**, (12), pp. 4154–4167
3 Sanchez, P.C., Mingo, J., Ducar, P.G., Carro, G., and Valdovinos, A.: 'Figures of merit and performance measurements for RF and microwave tunable matching networks'. European Microwave Integrated Circuits Conf., Manchester, UK, 2011, pp. 402–405
4 Brannan, D.A., Esplen, M., and Gray, J.J.: 'Geometry' (Cambridge University Press, 2009)
5 Mukherjee, B., Prgati, P., and Mukherjee, J.: 'Hemispherical dielectric resonator antenna based on the Apollonian gasket of circles – a fractal approach', *IEEE Trans. Antennas Propag.*, 2014, **62**, (1), pp. 40–48
6 Muller, A.A., Soto, P., Dascalu, D., Neculoiu, D., and Boria, V.E.: 'A 3D Smith chart based on the Riemann sphere for active and passive microwave circuits', *IEEE Microw. Wirel. Lett.*, 2011, **2**, (6), pp. 286–288
7 Muller, A.A., Soto, P., Dascalu, D., and Boria, V.E.: 'The 3D Smith chart and its practical applications', *Microw. J.*, 2012, **5**, (7), pp. 64–74
8 Lucyszyn, S., and Robertson, D.I.: 'Monolithic narrow band filter using ultrahigh-Q tunable active inductors', *IEEE Trans. Microw. Theory Tech.*, 1994, **42**, pp. 2617–2622
9 Robertson, D.I., and Lucyszyn, S.: 'RFIC and MMIC design and technology' (IEE, London, UK, 2001)
10 Bario, S.C., Bahrmazy, P., Svendsen, S., Jagielski, O., and Pedersen, G. F.: 'Thermal loss in high-Q antennas', *Electron. Lett.*, 2014, **50**, (13), pp. 917–919